Journal of Solid Mechanics Vol. 11, No. 1 (2019) pp. 91-104
DOI: 10.22034/JSM.2019.664221

Fracture Parameters for Cracked Cylindrical Shells

M. Kadri [1,*], A. Sahli [2], S. Sahli [3]

[1]Laboratoire de Mécanique Appliquée, Université des Sciences et de la Technologie d'Oran , Algeria
[2]Laboratoire de Recherche des Technologies Industrielles, Université Ibn Khaldoun de Tiaret, Algeria
[3]Université d'Oran 2 Mohamed Ben Ahmed, Algeria

Received 27 September 2018; accepted 14 December 2018

ABSTRACT
In this paper, 2D boundary element stress analysis is carried out to obtain the *T*-stress for multiple internal edge cracks in thick-walled cylinders for a wide range of cylinder radius ratios and relative crack depth. The *T*-stress, together with the stress intensity factor *K*, provides a more reliable two-parameter prediction of fracture in linear elastic fracture mechanics. *T*-stress weight functions are then derived from the *T*-stress solutions for two reference load conditions corresponding to the cases when the cracked cylinder is subject to a uniform and to a linear applied stress variation on the crack faces. The derived weight functions are then verified for several non-linear load conditions. Using the BEM results as reference *T*-stress solutions; the *T*-stress weight functions for thick-walled cylinder have also been derived. Excellent agreements between the BEM results and weight function predictions are obtained. The weight functions derived are suitable for obtaining *T*-stress solutions for the corresponding cracked thick-walled cylinder under any complex stress fields. Results of the study show that the two dimensional BEM analysis, together with weight function method, can be used to provide a quick and accurate estimate of *T*-stress for 2-D crack problems.

Keywords : Fracture mechanics; *T*-stress; Contour integral approach; Thick-walled cylinders; Boundary element method.

1 INTRODUCTION

FRACTURE behaviour is generally characterized by a single parameter such as the stress intensity factors (SIFs) or path independent *J*-integral [1]. These quantities provide a measure of the dominant behaviour of the stress field in the vicinity of a crack-tip. In order to understand the effect of the structural and loading configuration on the 'constraint' [2] conditions at the crack-tip, another parameter is required. A second fracture parameter often used is the elastic *T*-stress. In two dimensions, the *T*-stress is defined as constant stress acting parallel to the crack and its magnitude is proportional to the nominal stress in the vicinity of the crack. Various studies have shown that the *T*-stress has significant influence on crack growth direction, crack growth stability, crack-tip constraint and fracture toughness [3-8]. In order to calculate the *T*-stress, researchers have used several techniques such as the stress substitution method [9], the variational method [10], the Eshelby *J*-integral method [11,12], the weight function method [13], the line spring method [14], the Betti–Rayleigh reciprocal theorem [15,16], and the interaction

*Corresponding author. Tel.: +213 55777900.
E-mail address: Mohammed84.kadri@univ-usto.dz (M. Kadri).

integral method [15,17]. The determination of the elastic *T*-stress for cracked geometries has been receiving much attention in recent years [16, 18-20]. This term corresponds to the second, non-singular term of William_s Eigen function expansion of the linear elastic stress field at the crack-tip [21]. It is increasingly being recognized as an important additional parameter besides the stress intensity factor for fracture mechanics analysis. Omission of the *T*-stress can, for example, lead to predicting substantially different extent of the plastic zone at the crack-tip, Larsson and Carlsson [9], Rice [22], as well as introducing significant errors in certain linear elastic fatigue crack-growth analysis, Suresh [23]. Several analytical and numerical schemes have been employed to evaluate the *T*-stress for cracked geometries. For example, Leevers and Radon [10] incorporated the Eigen functions into a variational formulation in elasticity and computed the coefficients of these Eigen functions directly. Kfouri [12], Nakamura and Parks [17] and Wang [19] used the interaction integral method, based on Eshelby_s theorem, in conjunction with the finite element method (FEM) while Sham [13] employed higher order weight functions to determine the *T*-stress term. Fett [18] has also developed Green's functions and has used the weight function approach with the method of boundary collocation for the evaluation of *T*-stresses for various cracked geometries. Sladek et al. [16] derived contour integrals based on Betti's reciprocal work theorem in two dimensions and implemented it together with the boundary element method (BEM) for fracture mechanics analysis; the work was recently being extended to three dimensions, Sladek and Sladek [24]. In order to apply this two-parameter fracture mechanics methodology, it is important to provide accurate stress intensity factor solutions and *T*-stress solutions for the crack problems of practical interests. Although several handbooks [25, 26] devoted solely to stress intensity factors have been published, the available solutions for *T*-stress are very limited. Several analytical and numerical methods were developed to obtain the *T*-stress for different test specimens. The closed-form *T*-stress solutions for infinite plate crack problems have been analytically obtained by [27] using complex potential theory. Based on Shelby's theorem, the interaction integral method, in conjunction with finite element method has been used by [19] to obtain the *T*-stress solutions for several commonly used test specimens under remote and crack face loading conditions. The boundary integral equation method, commonly known as the boundary element method (BEM), is an alternative to finite element method (FEM); it has distinct advantages in fracture mechanics analysis. Some researchers have explored formulas [28, 29] to obtain stress intensity factors using BEM. Unfortunately, the BEM solutions for *T*-stress are still very limited in literature. Recent work conducted by [30] has derived a direct approach, analogous to the displacement formula of stress intensity factor solution for plane crack problems. Sladek et al [20] developed an integral formula to calculate the *T*-stress on a contour away from the crack tip. The present study is the expansion of the two above-mentioned works to develop the T-stress solutions for 'low constraint' geometries, e.g. cracked thick-walled cylinders under different loading conditions.

In practice, the loading conditions of cracked components are usually quite complex. This can be due to the existence of residual stresses, stress concentrations, or thermal stresses. The weight function (WF) method, mathematically, the Green's function method, is one of the most efficient methods to derive stress intensity factor solutions for complex nonlinear stress distributions. This method has been extended by [19] to derive the *T*-stress solutions under complex stress conditions in his recent work using the finite element results. However, the weight function analysis of *T*-stress using the boundary element results as reference *T*-stress solutions has not yet been carried out previously. Hence, to derive the weight functions for cracked thick-walled cylinders using BEM solutions is a focus of the present study as well.

2 FRACTURE PARAMETERS: *T*-STRESS AND STRESS INTENSITY FACTORS

Williams' asymptotic solution [21] for crack-tip stress fields in any linear elastic body is given by a series of the form

$$\sigma_{ij} = A r^{-\frac{1}{2}} f_{ij}\left(\theta\right) + B r^{0} g_{ij}\left(\theta\right) + C r^{\frac{1}{2}} h_{ij}\left(\theta\right) + ... \tag{1}$$

where *r* and θ are polar coordinates centered at the crack tip, σ_{ij} is the stress tensor. The functions $f_{ij}\left(\theta\right), g_{ij}\left(\theta\right)$ and $h_{ij}\left(\theta\right)$ contain trigonometric functions of the angular location relative to crack tip. Parameters *A, B* and *C* are proportional to the applied load. As $r \rightarrow O$, the leading term dominates and exhibits $1/\sqrt{r}$ singularity, while the higher order terms remain finite values or approach zero. Therefore, the stress field near the crack tip is expressed in the following form by only involving the first singular tern of Eq. (1):

$$\sigma_{ij} = \frac{K_I}{\sqrt{2\pi r}} f_{ij}(\theta) \tag{2}$$

where K_I is the stress intensity factor. Over the past thirty years, increasing attention has been put to study the effect of higher order terms of Williams' series expansion on the initiation of mode I, fracture under predominantly linear elastic deformation. Larsson and Carlson [9] carried out investigation on elastic-plastic problem for cracks in different type of specimens using finite element method (FEM) and found that the solutions for the stress state near the crack tip cannot be related to Eq. (2) through the stress intensity factor K_I alone, even when the requirements for "small scale yielding' are all met. They noted that the discrepancies would be resolved if the first non-singular term of Williams' series expansion (Eq. (1)) is included in the near tip stress solution, which is,

$$\sigma_{ij} = \frac{K_I}{\sqrt{2\pi r}} f_{ij}(\theta) + T_{ij}\delta_{i1}\delta_{i1} \tag{3}$$

In fact, there is only one non-singular term in this expansion for the elastic stress field in mode I, namely, T_{11}. This represents the uniform stress acting parallel to the crack plane. In the notation of Rice [22], this second tern of Williams' series expansion is denoted as the *T*-stress or elastic *T*-stress. *T*-stress is directly proportional to the load applied to the cracked structure and depends on the geometrical parameters.

To normalize the effect of the *T*-stress relative to the stress intensity factor in mode I, Leevers and Radon [10] proposed a dimensionless parameter called the biaxiality ratio β, which is,

$$\beta = \frac{\left(T\sqrt{\pi a}\right)}{K_I} \tag{4}$$

where a is crack depth and K_I is mode I, stress intensity factor. The stress field variation and fracture toughness discrepancies due to geometric differences are usually caused by the different 'constraint' effects in various specimen geometries. For so-called 'high constraint' geometries, such as compact tension and three point bending specimens, a single parameter K_c was able to fully describe the stress field and fracture properties; whereas for "low constraint" geometries, such as center cracked and double edge cracked specimens, the fracture toughness estimated would be lower than its actual value.

The constraint effect could be better incorporated into fracture mechanics evaluation by the elastic *T*-stress. Work by [23] indicated that the sign and magnitude of *T*-stress could substantially change the level of crack tip stress triaxiality, hence influence crack tip constraint. Positive *T*-stress enhances the level of crack tip stress triaxiality and leads to high crack tip constraint; while negative *T*-stress reduce the level of crack tip stress triaxiality and leads to the loss of crack tip constraint. The works by [7, 31-33], further indicated that the *T*-stress, in addition to the stress intensity factor K_I, provides a more appropriate two-parameter characterization of plain strain elastic-plastic crack tip fields in a variety of crack configurations and loading conditions.

3 BOUNDARY ELEMENT METHOD (BEM) FOR FRACTURE MECHANICS

The displacement boundary integral equation (or conventional BIE (CBIE)) relating the boundary displacements $u_j(P)$ with the boundary tractions $t_j(P)$ in the absence of body forces can be written as:

$$C_{ij}\left(P_0\right)u_j(P_0) = \int_{\Gamma}\left[U_{ij}(P,P_0)t_j(P) - T_{ij}(P,P_0)u_j(P)\right]d\Gamma(P) \tag{5}$$

where *i,j* denote Cartesian components; and $T_{ij}(P,P_0)$ and $U_{ij}(P,P_0)$ represent the traction and displacement fundamental solutions at a boundary point P_0 due to a unit load placed at location *P*. The term $C_{ij}\left(P_0\right)$ is generally a function of the geometry variation at the boundary point P_0. Providing that P_0 is a smooth boundary point, that is, the outward normal vector to the boundary is continuous at P_0, then it can be shown that $C_{ij}\left(P_0\right)=1/2\delta_{ij}$ [34].

3.1 Direct approach for T-stress evaluation using BEM

A simple formula for obtaining the elastic *T*-stress using boundary element method (BEM) fracture mechanics analysis is presented by [30]. It is obtained by comparing the displacement variation on the 'quarter-point crack-tip boundary element' with the classical field solutions.

The displacements and stress field in the vicinity of crack tip are proportional to √r and 1/√r respectively. In order to obtain the correct variation of the field parameters, alternative shape functions have been introduced [35, 36 and 37] respectively. [38 and 39] have show, however, that by moving the mid-side node of a quadratic element to a quarter point position as shown in Fig. 1, the desired √r variation for displacement can be achieved.

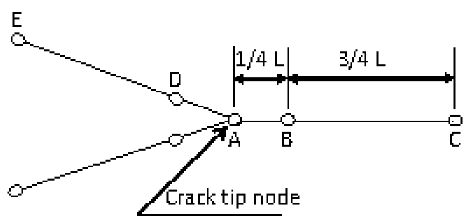

Fig.1
Node symbols for quarter-point crack type element.

Let $x^A=0, x^B=L/4$ and $x^C=L$ (for $y=0$) where L is the length of the element. Superscripts denote the nodes in Fig. 1. The coordinate x becomes:

$$x=\frac{1}{2}\xi(1+\xi)L+\frac{1}{4}(1-\xi^2) \tag{6}$$

Expressing ξ in terms of x, result in the following:

$$\xi=-1+2\sqrt{\frac{x}{L}}=-1+2\sqrt{\frac{r}{L}} \tag{7}$$

The displacements along a quarter-point element can be written as:

$$u_i=u_i^A+(-3u_i^A+4u_i^B-u_i^C)\sqrt{\frac{r}{L}}+2(u_i^A-2u_i^B+2(u_i^A-2u_i^C)\frac{r}{L} \tag{8}$$

Williams' series expansion (Eq. (1)) represents the classical solution for the elastic stress in the vicinity of a crack-tip. The corresponding displacement can be written, for plane strain, as:

$$u_1=\frac{K_I}{4\mu}\sqrt{\frac{r}{2\pi}}f_1(\theta)+\frac{K_{II}}{4\mu}\sqrt{\frac{r}{2\pi}}f_2(\theta)+(1-\nu^2)\frac{Tr}{E}\cos\theta \tag{9a}$$

$$u_2=\frac{K_I}{4\mu}\sqrt{\frac{r}{2\pi}}f_3(\theta)+\frac{K_{II}}{4\mu}\sqrt{\frac{r}{2\pi}}f_4(\theta)-\nu(1+\nu)\frac{Tr}{E}\sin\theta \tag{9b}$$

where μ is the shear modulus, E is the Young's modulus and υ is Poisson's ratio. The displacement formula for the computation of the stress intensity factor K_I have been obtained by equating the coefficient of the $\sqrt{r}$ term in Eq. (8) to the classical solutions in Eqs. (9a),(9b). An analogous formula can be obtained for elastic *T*-stress by comparing the coefficient of r term in Eq. (8) with that in Eq. (9a). The displacements of the quarter-point crack-tip element on the crack face with $\theta = 180^\circ$ can be written as:

$$2(u_i^A - 2u_i^B + u_i^C)\frac{1}{L} = -(1-\nu^2)\frac{T}{E} \tag{10}$$

which results in

$$T = -\frac{2E}{(1-\nu^2)L}(u_i^A - 2u_i^B + u_i^C) \tag{11}$$

The T-stress can then be evaluated directly from BEM computed nodal displacements on crack face quarter point element.

3.2 Contour integral approach for T-stress evaluation using BEM

An alternative approach of obtaining the elastic T-stress was introduced by Sladek et al. [16]. This is based on Betti-Rayleigh's reciprocal work theorem and some auxiliary fields. A contour integral formula is obtained which can evaluate T-stress along a closed path remote from the crack-tip, thus circumventing the more difficult task of establishing the accurate crack-tip fields and eliminating the numerical errors for near field solution associated with the crack-tip stress singularity. The required field variables along the integration path are obtained from the BEM analysis.

Consider a cracked isotropic, elastic domain R shown in Fig. 2 enclosed by the boundary S. Inside this domain, a closed integration path composed of Γ_0, Γ_c^+, and Γ_c^- is considered. For two sets of equilibrium states of the sub-domain, using Gauss's divergence theorem, Hooke's law and strain-displacement relation equations, Betti-Rayleigh's reciprocal work theorem can be written as:

$$\int_\Gamma \left(\sigma_{ij} u_i' n_j - \sigma_{ij}' u_i n_j\right) d\Gamma = \int_\Omega \left(X_i' u_i - X_i u_i'\right) d\Omega \tag{12}$$

where X_i and X_i' are body forces in two load states respectively; and n_j is the outward normal at the contour Γ of integration sub-domain Ω.

Because of the stress singularity at the crack-tip, a small circular region bounded by r, in the vicinity of the crack-tip has to be excluded, as shown in Fig. 2. The radius ε is considered to be very small and is shrunk to zero in the limiting process. Contour $\Gamma = \Gamma_0 + \Gamma_c^+ + \Gamma_c^- - \Gamma_\varepsilon$, is a closed integration path in the anticlockwise direction. With no loss of genera1ity, assume that in Eq. (12), the primed state corresponds to an auxiliary field. The non-primed state corresponds to the unknown field. Assume an auxiliary field where $\sigma_{ij}' = 0$ on crack faces and body forces $X_i' = 0$. Eq. (12) can then be written as:

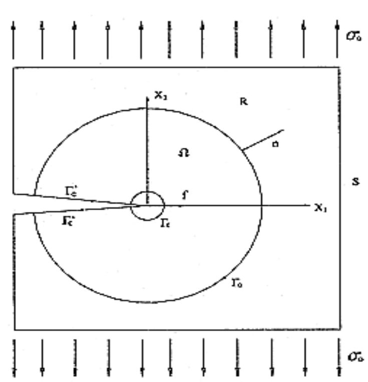

Fig.2
Integration paths and coordinate definitions.

$$\lim_{\varepsilon\to 0}\int_{\Gamma_\varepsilon}\left(\sigma_{ij}u_i^{'}n_j-\sigma_{ij}^{'}u_i n_j\right)d\Gamma=\int_{\Gamma_0}\left(\sigma_{ij}u_i^{'}n_j-\sigma_{ij}^{'}u_i n_j\right)d\Gamma-\int_{\Gamma_c^+}\left(\sigma_{ij}^{+}u_i^{'}n_j^{+}-\sigma_{ij}^{-}u_i^{'}n_j^{-}\right)\Gamma-\lim_{\varepsilon\to 0}\int_{\Omega-\Omega_\varepsilon}X_{,i}u_i^{'}d\Omega \tag{13}$$

where n_J^+ and n_J^- are outward normal vectors on upper and lower crack face respectively, and $n_J^+=-n_J^-$. For small equilibrium stress loads, assume $\sigma_{ij}^+=\sigma_{ij}^-$. Using the familiar relationship between traction and stresses $t_i=\sigma_{ij}n_{j,}$, Eq. (13) can be re-written as:

$$\lim_{\varepsilon\to 0}\int_{\Gamma_\varepsilon}\left(t_i^{'}u_i-t_i u^{'}\right)d\Gamma=\int_{\Gamma_0}\left(t_i^{'}u_i-t_i u^{'}\right)d\Gamma-\int_{\Gamma_c^+}2t_i^{+}u^{'}d\Gamma-\lim_{\varepsilon\to 0}\int_{\Omega-\Omega_\varepsilon}X_{,i}u_i^{'}d\Omega \tag{14}$$

By choosing different auxiliary fields, the Eq. (14) can be employed to derive integral formulas for computing various fracture parameters, For instance, Buecker [40] selected singular auxiliary fields to derive the integral expression for stress intensity factor K_I. In order to obtain a non-vanishing contribution of the elastic *T*-stress, and at the same time, eliminate the contribution due to singular integrand tern, a special auxiliary field solution has to be found. Sladek et al. [16] suggested a auxiliary field that has one order higher singularity than that used by [41]. The auxiliary displacements and tractions are proportional to r^{-1} and r^{-2} respectively; they are actually obtained by differentiating auxiliary field proposed by [41] with respect to X_I. The exact expression of the auxiliary field is,

$$\begin{aligned}
u_1^{'}(r,\theta)&=-\frac{f}{\pi Er}(1-\nu^2)\left(\cos\theta-\frac{1}{1-\nu}\sin^2\theta\cos\theta\right)\\
u_2^{'}(r,\theta)&=-\frac{f}{2\pi Er}(1+\nu)\left(1-2\nu-\cos 2\theta\right)\left(-\sin\theta\right)\\
\sigma_{11}^{'}(r,\theta)&=\frac{f}{\pi r^2}\cos^2\theta\left(\cos^2\theta-3\sin^2\theta\right)\\
\sigma_{12}^{'}(r,\theta)&=\frac{f}{\pi r^2}\sin 2\theta\cos 2\theta\\
\sigma_{22}^{'}(r,\theta)&=\frac{f}{\pi r^2}\sin^2\theta\left(3\cos^2\theta-\sin^2\theta\right)
\end{aligned} \tag{15}$$

where f is a static point force (see Fig.2) applied to the crack tip in the direction parallel to the crack plane. The unknown asymptotic displacements and stresses can be divided into two parts

$$u_i=u_i^s+u_i^T \tag{16}$$

$$\sigma_{ij}=\sigma_{ij}^s+\sigma_{ij}^T \tag{17}$$

where terms with superscript s are associated with the singular stress field and they correspond to first terns of Eqs. (9a),(9b) and Eq. (2), respectively those with superscript *T* are

$$\sigma_{ij}^T=T\,\delta_{i1}\delta_{j1} \tag{18}$$

$$u_i^T=\frac{Tr}{E}\left[\delta_{i1}\left(1-\nu^2\right)\cos\theta-\delta_{j2}\nu\left(1+\nu\right)\sin\theta\right] \tag{19}$$

Substituting the above auxiliary field solution and second term of Williams series expansion (*T*-stress term) into the left hand side of Eq. (14), gives

$$\lim_{\varepsilon\to 0}\int_{\Gamma_\varepsilon}\left(t_i^{'}u_i^T-t_i^T u^{'}\right)d\Gamma=\frac{1-\nu^2}{E}Tf \tag{20}$$

Substituting Eq. (15) and the singular terms u_i^s and t_i^s into the left hand side of Eq. (14), gives a vanishing contribution as:

$$\lim_{\varepsilon \to 0} \int_{\Gamma_\varepsilon} \left(t_i^{'} u_i^s - t_i^s u^{'} \right) d\Gamma = 0 \tag{21}$$

By further substituting Eq. (20) and Eq. (21) into Eq. (14), the integral representation of *T*-stress can finally be derived as follows:

$$T = \frac{E}{f\left(1-\nu^2\right)} \int_{\Gamma_0} \left(t_i^{'} u_i - t_i u^{'} \right) d\Gamma - \frac{2E}{f\left(1-\nu^2\right)} \int_{\Gamma_c^+} t_i^+ u^{'} d\Gamma \tag{22}$$

when body forces are absent. Furthermore, it can be proved that for mode I, cracked problems, even with non-zero crack face traction in the X_2 direction, the second term of Eq. (22) is always zero. So the general contour integral formula for *T*-stress, in the absence of body force, can then be expressed as:

$$T = \frac{E}{f\left(1-\nu^2\right)} \int_{\Gamma_0} \left(t_i^{'} u_i - t_i u^{'} \right) d\Gamma \tag{23}$$

It would be more explicit if Eq. (15) is substituted into the above equation. The *T*-stress expression is as follows:

$$T = \frac{E}{f\left(1-\nu^2\right)} \int_{\Gamma_0} \frac{f}{\pi r^2} \left(F_{ij}(\theta) u_i - t_i \frac{F_{ij}(\theta)}{E} \right) d\Gamma \tag{24}$$

where the function $F_{ij}(\theta)$ contain trigonometric functions of the angular location. The above integral expression can be numerically evaluated by using Gaussian quadrature scheme. The corresponding nodal parameters u_i and t_i along the integration path can be obtained from BEM analysis.

3.4 Weight function for T- stress

For mode I, crack problems, using the superposition method, it has been demonstrated by [19] that for a cracked body, loaded by stress field *Q*, the *T*-stress is the superposition of *T*-stresses for two cases:

The first is the *T*-stress for the same cracked body loaded by the crack face pressure $\sigma(x)$, which is induced by the stress field *Q* in the uncracked body.

The second case is the *T*-stress in the uncracked body under stress field *Q*.

Therefore, the *T*-stress for the problem can be calculated from the summation of the *T*-stress for these two sub-problems,

$$T_{remote\ loading} = T_{crack\ face\ pressure} + T_{uncracked} \tag{25}$$

Note the regular stress field has no singularity at the crack tip element, the corresponding stress intensity factor is zero. However, the *T*-stress has a finite value. The corresponding *T*-stress for the regular field is [19],

$$T_{uncracked} = \left(\sigma_x - \sigma_y \right)_{crack\ tip} \tag{26}$$

The *T*-stress for a cracked body with loading applied to the crack face can again be calculated by integrating the product of the weight function $t(x,a)$ and the stress distribution $\sigma(x)$ on the crack face,

$$T_{crack\ face\ pressure} = \int_0^a \sigma_x t(x,a)dx \tag{27}$$

where $t(x,a)$ is the weight function for *T*-stress. Similar to the weight functions for the stress intensity factor, the weight function for *T*-stress is also only dependent on crack geometry and is independent of the loading conditions. The weight function $t(x,a)$, is the Green's function for the *T*-stress. It represents the *T*-stress at the crack tip for a pair of unit loads acting along the crack face as the location *x*.

Substituting Eq. (26) and Eq. (27) into Eq. (25), the *T*-stress for the cracked body, loaded by a stress field *Q*, is obtained,

$$T_{remote\ loading} = \int_0^a \sigma_x t(x,a)dx + \left(\sigma_x - \sigma_y\right)_{crack\ tip} \tag{28}$$

Eq. (28) provides a very efficient way for *T*-stress calculation for arbitrary load situations. Once the weight function $t(x,a)$ is determined, and a stress analysis of uncracked body is conducted to obtain $\left(\sigma_x - \sigma_y\right)_{crack\ tip}$ and $\sigma(x)$, the corresponding *T*-stress can be calculated for any arbitrary loading conditions. Several authors have proposed different approaches to obtain weight functions for *T*-stress. For example, Sham [13] has provided numerical methods for the determinations of weight functions for *T*-stress. In the other researches [19, 42 and 43] proposed different methods for the derivation of weight functions from reference *T*-stress solutions.

4 CRACKED THICK-WALLED CYLINDERS

In practice, failure of thick-walled pressurized cylinders (e.g. gun tubes, pipes and pressure vessels) is often due to the presence of internal or external cracks. A long internal single radial crack may be treated as a through crack in two-dimensions and is commonly seen in such components. Generally, cracked cylinders under internal pressure can be considered as "low-constrained" geometries. Thus the fracture toughness measured from "high-constrained" test specimens, such as compact tension and three-point bending specimens may be conservative when applied to this geometry. Therefore, accurate *T*-stress solutions for thick-walled cylinder with internal radial crack are needed to reliably predict the failure loads. Unfortunately, these solutions are not available in the literature at present.

The purpose of this section is to extend the BEM analysis to thick-walled cylinders to obtain the *T*-stress solutions using both the direct approach as well as the contour integral approach, as before. At the same time, the stress intensity factor solutions were also calculated and compared to the published results in the literature [44, 45] to verify the accuracy of the BEM model.

To facilitate the *T* -stress calculations for more complex loading conditions, for example, high residual stresses, stress concentrations or thermal stress, the weight function for *T* -stress needs to be developed. The two-term weight function approximation proposed by [19] is used to obtain the *T*-stress in cracked thick-walled cylinders. The BEM solutions under constant and linear crack face loading conditions are fitted with empirical formulas, which are then used to obtain the coefficients of weight functions. Finally, the weight functions are verified using *T* -stress solutions for internal pressure, parabolic and cubic stress distributions on the crack face obtained directly.

4.1 Numerical modeling

A thick-walled cylinder with an internal single radial crack, as shown in Fig. 3, was analysed in this study. The geometry of the cylinder in the x_1, x_2 plane was defined by relative crack length a/W and R_0/R_i ratio, where $W = R_0 - R_i$. As before, plane strain conditions are assumed in the analysis. All BEM analysis were carried out using the computer program BEMC2D which have developed by Professor O. Rahmani at USTO MB University. Two separate FORTRAN subroutines for calculating the *T*-stress directly based on the above two BEM approaches were developed.

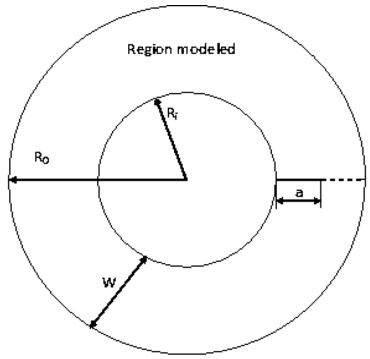

Fig.3
A thick walled cylinder with a single radial crack.

In this study, the relative crack length was varied with a/W = 0.1, 0.2, 0.3, 0.4, 0.5 and 0.6. For a given a/W ratio, the following radius ratios were analysed, R_0/R_i = 1 5, 1.75, 2.0, 2.25 and 2.5 to investigate the effect of wall thickness on the *T*-stress. Different load conditions were also investigated. Uniform internal pressure, *p,* was first applied, then, as before, the four types of basic crack face loading conditions corresponding to *n=0* to 3 in the following stress distribution:

$$\sigma(x_1) = \sigma_0 \left(1 - \frac{x_1}{a}\right)^n \tag{29}$$

were analysed, where σ_0 is the nominal stress, *a* is the crack length, they correspond to the uniform, linear, parabolic and cubic crack face loading, respectively.

Because of symmetry, only one-half of the physical problems need to be modeled (even if the cracks are symmetrically formed in the cylinder). A typical BEM model is presented in Fig. 4. The following boundary conditions were applied: along the horizontal plane of symmetry, elements in the uncracked ligament were constrained in the x_2 direction, but were free to displace in the x_1 direction. Also, one node along the plane symmetry was constrained in x_1 direction to prevent rigid body motion in that direction. As before, quarter-point elements were used for those elements adjacent to the crack-tip. For the contour integral approach to obtain the *T*-stress, an integration path, Γ_0, with relative radius $r/a = 0.5$ as shown in Fig. 4 was employed for both internal pressure and crack face loading conditions.

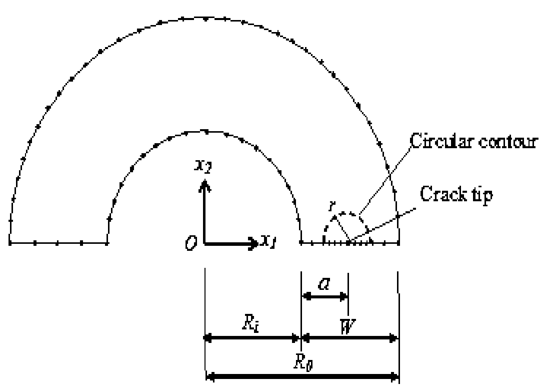

Fig.4
Typical boundary element mesh for thick walled cylinder.

4.2 BEM results and discussions

T-stress solutions obtained in the analysis were normalized as follows:

$$T^* = \frac{T}{\sigma_0} \tag{30}$$

where σ_0 is the nominal stress for crack face loading case, and equals p in the internal pressure case. For the internal pressure case, the normalized values of T^* are obtained using both direct approach and contour integral approach and shown in Figs. 5 and 6 for the radius ratios $R_0 / R_i = 2.0$ and 2.25. It can be seen that the discrepancies of the solutions obtained using this two approaches varied from 5% to 10%. From model verification, the contour integral solutions can be considered as more stable and accurate results. For the crack face loading cases, the normalized *T*-stress solutions under uniform, linear, parabolic and cubic crack face loading are shown in Figs. 5 and 6. It can be seen that all the *T*-stress values for each of the different crack face loading conditions show a trend of decreasing value with the relative crack length from $a/W = 0.1$ to 0.6. This suggests that deeply cracked thick walled cylinders have lower constraint effects at the crack tip when compared with those with shallow cracks under crack face loading. From these figures, it can also be seen that, compared to non-linear crack face loading (e,g, parabolic and cubic) conditions, the *T*-stress curves under the uniform and linear crack face loading conditions show relatively steeper declines when the crack length grows. This implies that the cracked cylinders with lower constraint conditions can be more easily obtained under uniform and linear crack face loading conditions increasing crack length.

In order to better demonstrate the effects of radius ratio, R_0 / R_i , on the *T*-stress solutions, these *T*-stress data for internal pressure and the four types of crack face loading conditions were re-organized and re-plotted in Fig. 7 and Fig. 8, respectively. The *T*-stress solutions under crack face loading showed a decreasing trend when R_0 / R_i varied from 1.5 to 2.5. On the other hand, the *T*-stress results for internal pressure showed a trend of increasing value when R_0 / R_i increased from 1.5 to 2.5. These figures also showed that the effect of radius ratio R_0 / R_i on *T*-stress is more evident when the relative crack length increased.

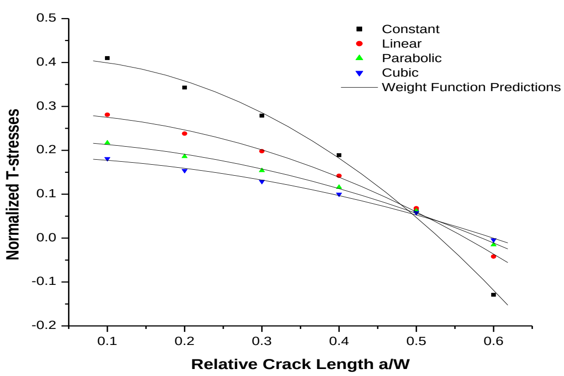

Fig.5
Comparison of nomalized BEM *T*-stresses and weight function predictions for thick-walled cylinder with internal single radial crack under different crack face loading ($R_0 / R_i = 2.0$).

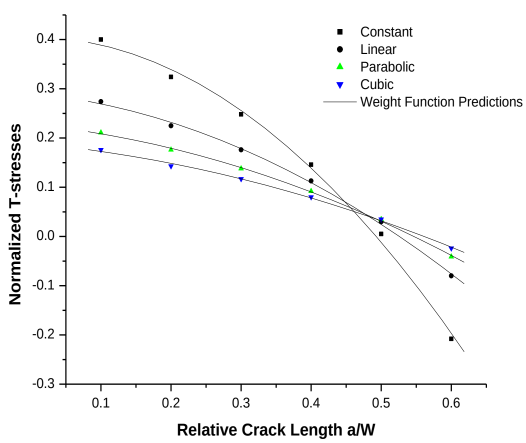

Fig.6
Comparison of normalized BEM *T*-stresses and weight function predictions for thick-walled cylinder with internal single radial crack under different crack face loading ($R_0 / R_i = 2.25$).

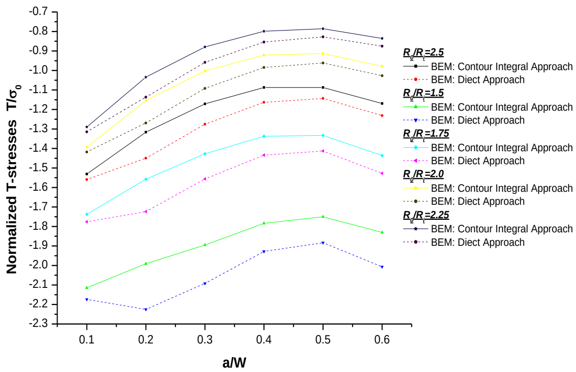

Fig.7
Comparison of normalized *T*-stresses, T / σ_0, between BEM contour integral approach and BEM direct approach for different relative crack lengths, a / W, thick-walled cylinder under internal pressure loading.

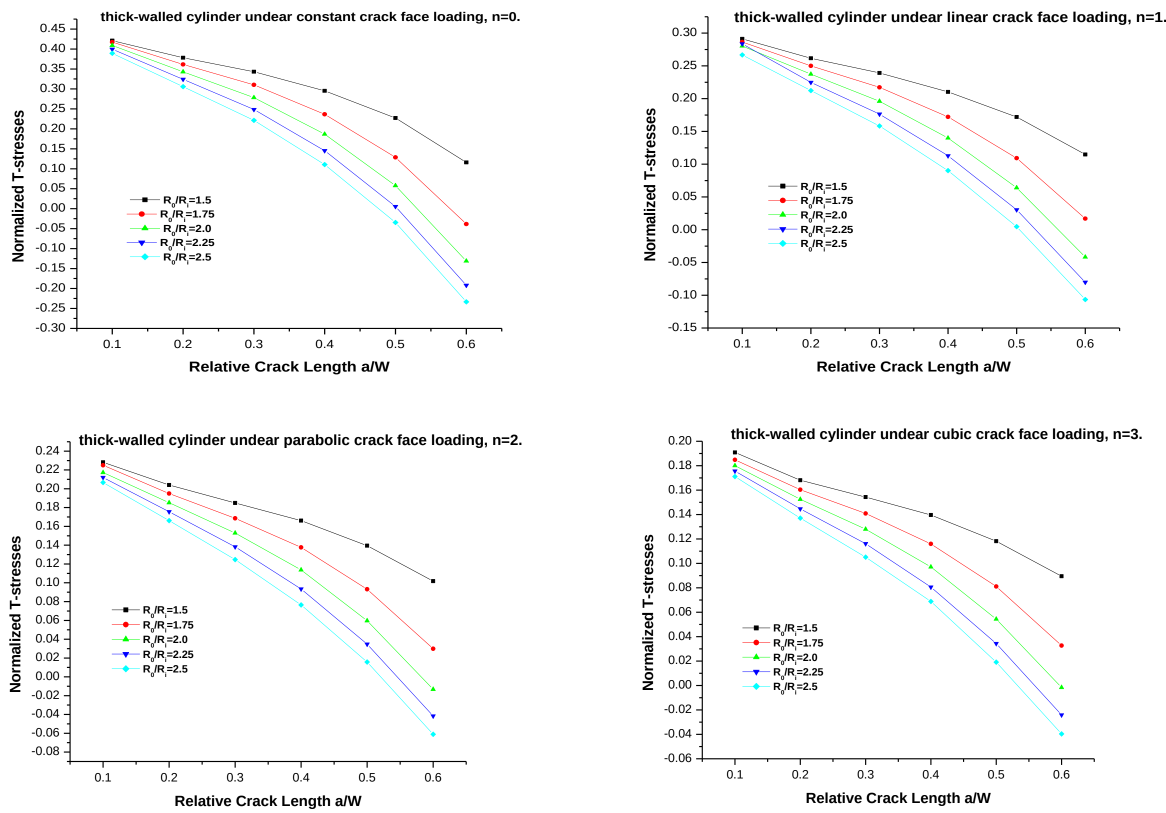

Fig.8
Normalized *T*-stresses for thick-walled cylinder under crack face loading.

For the purpose of validating the BEM model of thick-walled cylinder, the stress intensity factors were first calculated. The stress intensity factor were nomalized as follows:

$$K_I^* = \frac{K_I}{\sigma_0 \sqrt{\pi a}} \tag{31}$$

The normalized stress intensity factor results under internal pressure are presented in Fig. 9 and compared with the solutions from Wu and CarIsson (1991). The largest discrepancy was found to be only 1.2%.

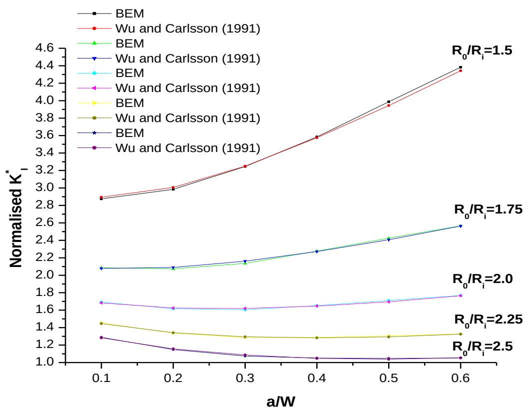

Fig.9
Comparison of normalized stress intensity factor solutions, $K_I^* = K_I / \sigma_0 \sqrt{\pi a}$ from present BEM analysis and solutions by Wu and Carlsson (4994): thick- walled cylinder under internal pressure, $\sigma_0 = p$.

The normalized stress intensity factors for crack face loading, i.e. constant, linear, parabolic and cubic load cases, with the wall thickness ratio $R_0 / R_i = 1.75$ were also obtained and are shown in Table 1. In this Table, comparison between the BEM stress intensity factor solutions and those from Andrasic and Parker [44] using modified mapping collocation (MMC) technique are also presented. The percentage differences are generally less than 2% - The excellent agreement between the current BEM stress intensity factor solutions and these numerical results in the literatures demonstrated the reliability of the current BEM model for thick-walled cylinder analysis.

Table1
Comparison of normalized stress intensity factor solutions, $K_I^* = K_I / \sigma_0 \sqrt{\pi a}$ from present BEM calculation and solutions by Andrasic and Parker [44], thick-walled cylinder under cubic crack face loading, $R_0 / R_i = 1.75$.

a/W	n=0		n=1		n=2		n=3	
	K_I^* BEM	K_I^* [44]	K_I^* BEM	K_I^* [44]	K_I^* BEM	K_I^* [44]	K_I^* BEM	K_I^* [44]
0.1	1.129	1.127	0.442	0.441	0.283	0.282	0.212	0.209
0.2	1.189	1.2	0.48	0.485	0.314	0.314	0.232	0.235
0.3	1.286	1.3	0.54	0.547	0.362	0.359	0.266	0.269
0.4	1.427	1.427	0.63	0.625	0.417	0.416	0.319	0.314
0.5	1.577	1.563	0.715	0.708	0.48	0.476	0.366	0.361
0.6	1.725	1.718	0.804	0.801	0.544	0.542	0.413	0.413

5 CONCLUSIONS

Two-dimensional BEM *T*-stress analysis of thick-walled cylinders with different R_0 / R_i ratios and loading conditions were analysed for a range of relative crack lengths, a/W , varying from 0.1 to 0.6, These results are new and have not been available previously in the literature. They can be used for failure assessment analysis of cracked thick-walled cylinders, For internal pressure case, *T*-stress solutions show a typica1 ″low constraint″ effect. The *T*-stress weight functions for cracked thick walled cylinders with different radius ratio have also been derived. The weight function technique has been verified by using the BEM *T*-stress solutions for crack face loading conditions and internal pressure case. All the comparisons demonstrate the reliability of weight function method in engineering *T*-stress analysis.

The following general conclusions can be made from the analyses conducted in this study. First, the crack tip element size is a critical parameter which affects the accuracy of the BEM direct displacement approach *T*-stress solutions. Generally, a crack tip element size of 5% of the crack length can limit the numerical error of the *T*-stress obtained to be within 5%.

Second, because the computations in the contour integral approach are carried out away from crack tip, it is numerically more stable and accurate than direct approach in BEM *T*-stress analysis. The results are generally independent of the contour size and geometry. By choosing a circular contour with radius which equals half of the crack length, the numerical results for *T*-stress were generally less than 2% in discrepancy with those in the literature using the finite element method and with the BEM direct approach. Third, the thick-walled cylinder exhibits typical “low constraint” characteristics under internal pressure loads. For decreasing crack face loading conditions, the 'low constraint' effect is more obvious with deeper cracks. This indicates that using the two-parameter fracture mechanics, which include the constraint effect, will likely lead to less conservative life prediction in service.

REFERENCES

[1] Rice J.R., 1968, Path-independent integral and the approximate analysis of strain concentration by notches and cracks, *Journal of Applied Mechanics* **35**(2): 379-386.

[2] Anderson T.L., 1995, *Fracture Mechanics: Fundamentals and Applications*, Boca Raton, CRC Press.

[3] Williams J.G., Ewing P.D., 1972, Fracture under complex stress—the angled crack problem, *International Journal of Fracture* **8**(4): 416-441.

[4] Ueda Y., Ikeda K., Yao T., Aoki M., 1983, Characteristics of brittle failure under general combined modes including those under bi-axial tensile loads, *Engineering Fracture Mechanics* **18**(6):1131-1158.

[5] Smith D.J., Ayatollahi M.R., Pavier M.J., 2001, The role of *T*-stress in brittle fracture for linear elastic materials under mixed-mode loading, *Fatigue & Fracture of Engineering Materials & Structures* **24**(2):137-150.

[6] Cotterell B., Rice J.R., 1980, Slightly curved or kinked cracks, *International Journal of Fracture* **16**(2):155-169.

[7] Du Z-Z., Hancock J.W., 1991, The effect of non-singular stresses on crack-tip constraint, *Journal of the Mechanics and Physics of Solids* **39**(3): 555-567.

[8] O'Dowd N.P., Shih C.F., Dodds Jr R.H., 1995, The role of geometry and crack growth on constraint and implications for ductile/brittle fracture, In: Constraint effects in fracture theory and applications, *American Society for Testing and Materials* **2**:134-159.

[9] Larsson S.G., Carlson A.J., 1973, Influence of non-singular stress terms and specimen geometry on small-scale yielding at crack tips in elastic–plastic materials, *Journal of the Mechanics and Physics of Solids* **21**(4): 263-277.

[10] Leevers P.S., Radon J.C.D., 1982, Inherent stress biaxiality in various fracture specimen, *International Journal of Fracture* **19**(4): 311-325.

[11] Cardew G.E., Goldthorpe M.R., Howard I.C., Kfouri A.P., 1985, *Fundamentals of Deformation and Fracture*, Eshelby Memorial Symposium Sheffield.

[12] Kfouri A.P., 1986, Some evaluations of the elastic *T*-term using Eshelby's method, *International Journal of Fracture* **30**(4): 301-315.

[13] Sham T.L., 1991, The determination of the elastic *T*-term using higher-order weight functions, *International Journal of Fracture* **48**(2):81-102.

[14] Wang Y-Y., Parks D.M., 1992, Evaluation of the elastic *T*-stress in surface cracked plates using the line-spring method, *International Journal of Fracture* **56**(1): 25-40.

[15] Chen C.S., Krause R., Pettit R.G., Banks-Sills L., Ingraffea A.R., 2001, Numerical assessment of *T*-stress computation using a *p*-version finite element method, *International Journal of Fracture* **107**(2):177-199.

[16] Sladek J., Sladek V., Fedelinski P., 1997, Contour integrals for mixed-mode crack analysis: effect of nonsingular terms, *Theoretical and Applied Fracture Mechanics* **27**:115-127.

[17] Nakamura T., Parks D.M., 1992, Determination of *T*-stress along three dimensional crack fronts using an interaction integral method, *International Journal of Solids and Structures* **29**(13):1597-1611.

[18] Fett T., 2002, *T -Stress Solutions and Stress Intensity Factors for 1-D Cracks*, Dusseldorf, VDI Verlag.

[19] Wang X., 2002, Elastic *T*-stress for cracks in test specimens subjected to non-uniform stress distributions, *Engineering Fracture Mechanics* **69**: 1339-1352.

[20] Zhao L.G., Chen Y.H.,1996, On the elastic *T* -term of a main crack induced by near tip microcracks, *International Journal of Fracture* **82**: 363-379.

[21] Williams M.L., 1957, On the stress distribution at the base of a stationary crack, *Journal of Applied Mechanics* **24**:109-114.

[22] Rice J.R., 1974, Limitations to the small scale yielding approximation for crack tip plasticity, *Journal of the Mechanics and Physics of Solids* **22**:17-26.

[23] Suresh S., 1991, *Fatigue of Materials*, Cambridge University Press.

[24] Sladek J., Sladek V., 2000, Evaluation of the elastic *T* -stress in three-dimensional crack problems using an integral formula, *International Journal of Fracture* **101**: 47-52.

[25] Rooke D.P., Cright D.J., 1 976, *Compendium of Stress Intensity Factors,* Willingon Press.

[26] Tada H., Paris P.C., Mn G.R., 1984, *The Strew Analysir of Crarks Handbook ,* Paris Productions.

[27] Chen V.Z., 2000, Closed form solutions of *T*-stress in plate elasticity crack problems, *International Journal of Solid Structure* **37**: 1629-1637.

[28] Tan C.L., 1987, *The Boundary Element Method: A Short Course,* Carleton University, OMawa, Ontdo.

[29] Aliabadi M.W., Rooke D.P., 1991, *Numerical Fracture Mechanics,* Kluwer Aeademic Publishers, Boston.

[30] Tan C.L., Wang X., 2003, The use of quarter-point crack tip elements for *T*-stress determination in boundary element method (BEM) analysis, *Engineering Fracture Mechanics* **70**: 2247-2252.

[31] Betegon C., Hancock J.W., 1991, Two-parameter characterization of elastic-plastic crack tip field, *Journal of Applied Mechanics* **58**: 104-110.

[32] 0'Dowd N.P., Shih C.F., 1991, Family of crack tip fields characterized by a triaxiality parameter-I : Structure of fields, *Journal of the Mechanics and Physics of Solids* **24**: 989-1015.

[33] Wang Y.Y., 1993, *On the Two-Parameter Characterization of Elastic-Plastic Crack Front Fields in Surface Cracked Plates*, In: Hackett E.M., Schwalbe K.M., Dodds R.H., Editors.

[34] Sahli A., Rahmani O., 2009, Stress intensity factor solutions for two-dimensional elastostatic problems by the hypersingular boundary integral equation, *Journal of Strain Analysis* **44**(4): 235-247.

[35] Yamada U., Ezawa *Y.,* Nishiguchi I., 1979, Recommendations on singularity or crack tip elements, *International Journal of Mechanical Engineering* **14**: 1525-1544.

[36] Blackbum W.S., 1977, *The Mathematics of Finite Elements and Applications,* Brunel University.

[37] Akin J.E., 1976, The generation of elements with singularities, *International Journal of Mechanical Engineering* **10**: 1249-1259.

[38] Henshell R.D., Shaw K.G., 1975, Crack-tip finite elements are unnecessary, *International Journal of Mechanical Engineering* **9**: 495-507.

[39] Barsoum R.S., 1976, On the use of isoparametric finite elements in linear fracture mechanics, *International Journal of Mechanical Engineering* **10**: 25-37.

[40] Buecker H.F., 1989, A novel principle for the computation of stress intensity factor, *Zeitschrift für Angewandte Mathematik und Mechanik* **50**: 129-146.

[41] Kfouri A.P., 1986, Some evaluations of the elastic *T*-stress using Eshelby's method, *International Journal of Fracture* **20**: 301-315.

[42] Fett T., 1997, A Green's function for *T*-stress in an edge cracked rectangular plate, *Engineering Fracture Mechanics* **57**: 365-373.

[43] Hooton D.G., Sherry A.H., Sanderson D.J., Ainsworth R.A., 1998, Application of R6 constraint methods using weight function for *T*-stress, *ASME Pressure Vessel Piping Conference* **365**: 37-43.

[44] Andrasic C.P., Parker A.P., 1984, Dimensionless stress intensity factors for cracked thick cylinders under polynomial crack face loadings, *Engineering Fracture Mechanics* **19**: 187-193.

[45] Wu X.R., Carlsson A.J., 1991, *Weight Functions and Stress Intensity Factor Solutions,* Pergamon Press.